

Effects of disorder on the non-zero temperature Mott transitionM. C. O. Aguiar,¹ V. Dobrosavljević,² E. Abrahams,¹ and G. Kotliar¹¹*Center for Materials Theory, Serin Physics Laboratory, Rutgers University, 136 Frelinghuysen Road, Piscataway, New Jersey 08854, USA*²*Department of Physics and National High Magnetic Field Laboratory, Florida State University, Tallahassee, Florida 32306, USA*

(Received 7 February 2005; published 31 May 2005)

The physics of the metal-insulator coexistence region near the nonzero temperature Mott transition is investigated in presence of weak disorder. We demonstrate that disorder reduces the temperature extent and the general size of the coexistence region, consistent with recent experiments on several Mott systems. We also discuss the qualitative scenario for the disorder-modified Mott transition, and present simple scaling arguments that reveal the similarities to, and the differences from, the clean limit.

DOI: 10.1103/PhysRevB.71.205115

PACS number(s): 71.10.Fd, 71.30.+h, 71.55.Jv

I. INTRODUCTION AND MOTIVATION

The physics of the metal-insulator transition has continued to attract considerable interest in recent years. Substantial progress has been achieved in understanding the behavior near the interaction-driven transition, where dynamical mean field theory (DMFT) (Ref. 1) has been very successful in explaining the behavior of several classes of materials ranging from transition metal oxides such as V_2O_3 to organic Mott systems. This approach has been especially useful in describing the nonzero temperature behavior in the paramagnetic coexistence region between the metal and the insulator. In this regime, the two phases compete, and the resulting behavior emerges as a compromise between the energy gain to form coherent quasiparticles, and the larger entropy inherent to the incoherent insulating solution. There is not actual two-phase coexistence (as in conventional first-order thermodynamic phase transitions) in this region. Rather, it is a region of parameters in which two local minima of the free energy coexist.

So far, most theoretical work has concentrated on clean systems, although several experimental studies indicate that effects of disorder are particularly important precisely in this coexistence regime. Measurements performed in compounds such as NiSSe mixtures²⁻⁴ and κ -organics^{5,6} indicate that the presence of disorder pushes down the critical temperature end point of the metal and insulator coexistence region. In particular, experiments performed on a NiS₂ compound, which has much weaker disorder, show that the Mott transition occurs at 150 K,² with an external applied pressure of 3 GPa, while in the substituted NiS_{2-x}Se_x compound it is seen only below 100 K.⁴ It is important to notice that applying an external pressure to these compounds is equivalent to substituting S by Se, which might suggest that the results above would be in conflict. A speculation was made that the reduction in the transition temperature would be due to the local randomness introduced with Se substitution.³

We address the theoretical issues from the perspective of the Hubbard model. It is not *a priori* obvious what should be the effect of disorder on the size and the temperature range of the coexistence region. On the one hand, disorder tends to broaden the Hubbard bands and thus larger interaction is needed to open a Mott Hubbard gap. This may lead to a

larger overall energy scale, which could stabilize the coexistence region. On the other hand, disorder generally leads to spatial fluctuations in all local quantities, an effect that could smear or decrease the jump at any first order phase transition, and thus reduce the coexistence energy scale. These considerations indicate that careful theoretical work is called for, which can address the interplay of interactions and disorder near the Mott metal-insulator transition.

A formalism that describes the effects of disorder within a DMFT approach was outlined some time ago,⁷ but a very limited number of calculations were explicitly carried out within this framework. More recently, the approach was re-examined to investigate strong correlation effects on disorder screening,⁸ and the related temperature dependence of transport in the metallic phase.⁹ These results shed light on several puzzling phenomena observed in experiments on two dimensional electron systems, but did not provide a description of the physics relevant to the coexistence region at nonzero temperature.

In this paper, we examine the phase diagram for the Mott transition in the presence of moderate disorder at nonzero temperature within the DMFT approach.⁷ We present results describing the evolution of the coexistence region, showing that disorder generally reduces its size, in agreement with experiments. Our results give a physical picture that describes the gradual destruction of quasiparticles as the Mott insulator is approached, and establish the qualitative modification of the critical behavior resulting from the presence of disorder.

Our findings are valid in the regime of strong correlations but weak to moderate disorder, where Anderson localization effects, which are neglected in our theory, can be safely ignored. The latter have been included in earlier zero temperature DMFT-based strong correlation calculations.^{10,11} In particular, we mention that our lowest-temperature results are consistent with the $T=0$ result at weak disorder of Byczuk *et al.*,¹¹ but give the temperature dependence of the metal-insulator coexistence region.

II. NONZERO TEMPERATURE DMFT FOR DISORDERED ELECTRONS

We consider a half-filled Hubbard model in the presence of random site energies, as given by the Hamiltonian

$$H = -t \sum_{\langle ij \rangle \sigma} c_{i\sigma}^\dagger c_{j\sigma} + \sum_{i\sigma} \varepsilon_i n_{i\sigma} + U \sum_i n_{i\uparrow} n_{i\downarrow}. \quad (1)$$

Here $c_{i\sigma}^\dagger$ ($c_{i\sigma}$) creates (destroys) a conduction electron with spin σ on site i , $n_{i\sigma} = c_{i\sigma}^\dagger c_{i\sigma}$ is the particle number operator, t is the hopping amplitude, and U is the on-site repulsion. The random site energies ε_i are assumed to have a uniform distribution of width W .

Within DMFT for disordered electrons,⁷ a quasiparticle is characterized by a local but site-dependent¹² self-energy function $\Sigma_i(\omega) = \bar{\Sigma}(\omega, \varepsilon_i)$. To calculate these self-energies, the problem is mapped onto an *ensemble* of Anderson impurity problems⁷ embedded in a self-consistently calculated conduction bath. In this approach, only quantitative details of the solution depend on the details of the electronic band structure; in the following, we concentrate on a semicircular model density of states. In this particular case, the hybridization function is given by

$$\Delta(\omega) = t^2 \bar{G}(\omega) \quad (2)$$

and the average local Green's function, $\bar{G}(\omega)$, is obtained by imposing the following self-consistent condition

$$\bar{G}(\omega) = \left\langle \frac{1}{\omega - \varepsilon_i - \Delta(\omega) - \Sigma_i(\omega)} \right\rangle, \quad (3)$$

where $\langle \dots \rangle$ indicates the arithmetic average over the distribution of ε_i .

To solve the single-impurity problems at non-zero temperature for different site energies, we mostly used the iterated perturbation theory (IPT) method of Kajueter and Kotliar.^{13,14} However, to check the accuracy of the results, in several instances we also used the numerically exact quantum Monte Carlo method as an impurity solver, and generally found good qualitative and even quantitative agreement, supporting the validity of our IPT predictions in the relevant parameter ranges. Throughout the paper, we express all energies in units of the bandwidth.

III. PHASE DIAGRAM

We first examine the evolution of the coexistence region as disorder is introduced. Within this region, both metallic and insulating solutions are found, depending on the initial guess used in the iterative scheme for solving the self-consistency condition. Typical results are presented in Fig. 1, showing the phase diagram obtained within DMFT-IPT at nonzero temperature, for varying levels of disorder W . For each level of disorder [shown in panel (a)] or temperature [shown in panel (b)], the first (from left) of the two lines, the so-called U_{c1} , indicates the stability boundary (i.e., the spinodal) of the insulating solution. Conversely, the second of the two lines, identified as U_{c2} , represents the boundary of the metallic solution. The coexistence region is found between these two lines, i.e., for $U_{c1} < U < U_{c2}$. Our results are in good quantitative agreement with previous results obtained in the $T=0$ limit in presence of disorder,⁸ and also with non-zero temperature results in absence of disorder.¹ As the disorder increases, the metal-insulator transition generally

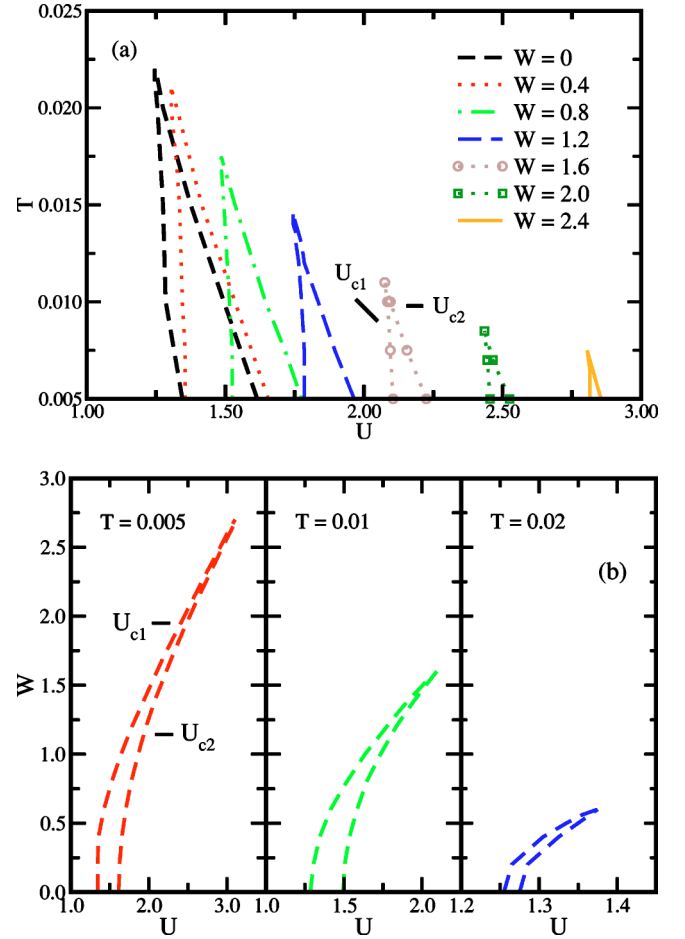


FIG. 1. (Color online) Phase diagram for the disordered Hubbard model at nonzero temperature. (a) (U, T) diagram for different disorder strengths. (b) (U, W) diagram at different temperatures. U_{c1} and U_{c2} lines are indicated in one of the plots, but similar definitions apply to the other results as well.

moves to larger U . Physically, this reflects the fact that disorder broadens the bands and smears the gap, making it harder for the Mott-Hubbard gap to open, so that a larger U is necessary for the transition. At the same time, the temperature-dependent coexistence region is found to shrink [Fig. 1(a)], persisting only below a critical end-point temperature $T_c(W)$. At any given temperature, the principal effects of introducing disorder [Fig. 1(b)] are as follows: (1) Both the U_{c1} and U_{c2} lines move toward larger interaction potential; and (2) the lines become closer to each other as disorder increases. In fact, they both approach the $W=U$ line as $W \rightarrow \infty$.

Having obtained these results in quantitative detail, we would like to understand the physical origin of this behavior. In the following, we present simple analytical arguments relating the nonzero temperature aspects of the coexistence region to the evolution of its ground state properties. Our strategy is motivated by the following observations: (a) The shape of the nonzero temperature coexistence region [Fig. 1(a)] remains *very similar* at different values of disorder; and (b) its size, both in terms of temperature and in terms of U range, shrinks as disorder increases. This suggests that the

physical mechanism for the destruction of the coexistence region as the temperature increases is similar to that of the clean limit, where it is governed by decoherence processes due to inelastic electron-electron scattering. Therefore, we begin our analysis by concentrating on the clean limit, where we show how simple estimates for the critical end-point temperature T_c can be obtained.

IV. COEXISTENCE REGION IN THE CLEAN LIMIT

The coexistence region at nonzero temperature is delimited by the two spinodal lines $U_{c1}(T)$ and $U_{c2}(T)$; the critical end-point temperature T_c is reached when these two boundaries intersect. To estimate T_c using the $T=0$ properties of the model, we need to understand the temperature dependence of each of these lines.

A. Insulating spinodal

The insulating spinodal $U_{c1}(T)$ essentially corresponds to the closing of the gap separating the two Hubbard bands in the Mott insulator. Its temperature dependence should thus reflect that of the Hubbard bands. In contrast to the correlated metallic state close to the Mott transition, the insulating solution is not characterized by a small energy scale in the coexistence region. Accordingly, it is not expected to have strong temperature dependence; its weak temperature dependence reflects activated processes across the Mott–Hubbard gap. Such activations only lead to (exponentially) weak rounding/broadening of the Hubbard bands, which should very slowly reduce $U_{c1}(T)$ as temperature increases. Such behavior is indeed clearly seen in our results. This temperature dependence is, however, much weaker than that characterizing $U_{c2}(T)$. For purposes of roughly estimating T_c , to leading order we can ignore this weak temperature dependence, so that

$$U_{c1}(T) \approx U_{c1}(T=0). \quad (4)$$

B. Metallic spinodal

In the vicinity of the Mott transition, the metallic solution is characterized by a low-energy scale corresponding to the coherence temperature T^* of a low-temperature Fermi liquid.¹ Above T^* , the heavy quasiparticles are destroyed, and the metallic solution becomes unstable. To estimate $U_{c2}(T)$, we need to determine how this coherence temperature varies as the transition is approached. From detailed studies of the clean¹ and disordered⁹ Hubbard models within DMFT, it is known that this coherence temperature can be estimated as

$$T^* \approx AT_F Z, \quad (5)$$

where T_F is the Fermi temperature, A is a constant of order one, and Z is the quasiparticle (QP) weight defined as

$$Z = \left[1 - \frac{\partial}{\partial \omega} \text{Im} \Sigma(\omega) \Big|_{\omega \rightarrow 0} \right]^{-1}. \quad (6)$$

The behavior of Z is well known in the clean limit,¹ where it decreases linearly as U increases toward the metallic spinodal, viz.

$$Z = C[U_{c2}(0) - U]. \quad (7)$$

From numerical studies,¹ the proportionality constant $C \approx 0.45$. Therefore, the coherence temperature can be written as

$$T^*(U) = ACT_F[U_{c2}(0) - U]. \quad (8)$$

We can now estimate the temperature dependence of $U_{c2}(T)$ as that value of the interaction needed to set $T^*(U) = T$, i.e.,

$$T = ACT_F[U_{c2}(0) - U_{c2}(T)].$$

In other words,

$$U_{c2}(T) \approx U_{c2}(0) - BT, \quad (9)$$

where $B = 1/ACT_F$. From our numerical results [see Fig. 1(a)], we find $B \approx 22$, giving $A \approx 0.2$, in reasonable agreement¹⁵ with estimates⁹ from the literature.

Using these expressions for $U_{c1}(T)$ and $U_{c2}(T)$, we arrive at the estimate for the critical end-point temperature

$$T_c \approx [U_{c2}(0) - U_{c1}(0)]/B, \quad (10)$$

which agrees within 10% with our numerical results (see Fig. 7).

V. CRITICAL BEHAVIOR IN PRESENCE OF DISORDER

Encouraged by the success of our analytical description of the coexistence regime in the clean limit, we now turn our attention to the effects of disorder. As in the clean limit, we would like to relate the finite temperature properties to the critical behavior of the quasiparticles at $T=0$. To do this, we therefore concentrate on describing the critical behavior in presence of disorder.

The principal new feature introduced by disorder within the DMFT scheme is the spatial variation of the spectral function, $\rho_i(\omega)$. This is shown in Fig. 2 at all energy scales: On the left we have the average spectral function, and on the right the relative deviation of its distribution, in the metallic phase. For each value of the interaction potential, the distribution of $\rho_i(\omega)$ presents a large dip at $\omega \approx 0$ and becomes broader as the frequency increases. This comes from the fact that at small frequencies the system is in the Fermi liquid regime. At finite temperature, we observe the reminiscence of the perfect disorder screening seen at $T=0$ close to the Mott transition.⁸ For large frequencies, the quasiparticle regime is no more valid and the appropriate description is in terms of Hubbard bands, resulting in an increase of the fluctuation in $\rho_i(\omega)$.

In the disordered case, the self-energy function $\Sigma_i(\omega)$ presents site-to-site fluctuations, which lead to the spatial variations of the spectral function discussed above. The QP weights $Z_i = Z(\varepsilon_i)$ now depend on the local site energy ε_i . To properly describe the approach to the Mott transition, we therefore must follow the evolution of the entire function $Z(\varepsilon_i)$ as the transition is approached.¹⁶

A. Behavior of local QP weights

Given the self-consistent solution of our ensemble of impurity models, we calculate the local QP weights as

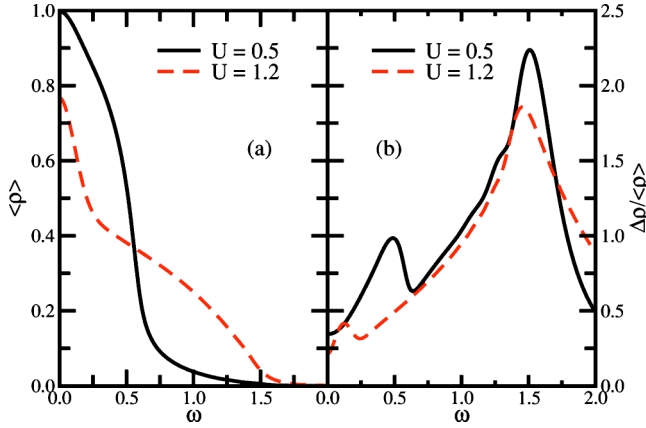


FIG. 2. (Color online) (a) Average spectral function and (b) relative deviation of the distribution of $\rho_i(\omega)$, $\Delta\rho/\langle\rho\rangle$, as a function of frequency for different values of the interaction potential. $\Delta\rho$ is the standard deviation of the distribution of $\rho_i(\omega)$, which is given by $\sqrt{\sum_i(\rho_i(\omega)-\langle\rho_i(\omega)\rangle)^2/(N-1)}$, where N is the number of local site energies considered. Other parameters used were $T=0.05$ and $W=1.0$.

$$Z_i = \left[1 - \frac{\partial}{\partial \omega} \text{Im} \Sigma_i(\omega) \Big|_{\omega \rightarrow 0} \right]^{-1}. \quad (11)$$

Typical results are shown in Fig. 3(a), where we plot $Z_i=Z(\varepsilon_i)$ at $T=0.005$, for disorder strength $W=1$, as the metallic spinodal is approached by increasing the interaction U toward $U_{c2} \approx 1.9$. We first observe that for small U , away from the transition, the QP weights Z_i have strong ε_i dependence, with the smallest Z_i at $\varepsilon_i=0$. Physically, this reflects the tendency for correlation effects (suppression of Z) to be the strongest on sites which are locally close to half-filling (singly occupied). Nonzero site energies favor the local occupation departing from half-filling, thus reducing the correlation effect, and increasing Z_i .

As U increases, all the Z_i 's decrease, as in the clean case. But how does this affect the distribution of QP weights $Z_i=Z(\varepsilon_i)$? At first glance, it seems that the ε_i dependence becomes weaker, but a closer look reveals this not to be the case. As we shall now demonstrate, all the Z_i 's decrease linearly near the transition, i.e., they assume the form

$$Z(U, \varepsilon_i) = K(\varepsilon_i)[U_{c2} - U], \quad (12)$$

where only the prefactor $K(\varepsilon_i)$ depends on ε_i . If, to leading order, these prefactors remain independent of the distance to the spinodal, then the entire family of curves $Z(U, \varepsilon_i)$ can all be collapsed on a single scaling function. To verify this hypothesis, we define reduced QP weights

$$Z^*(\varepsilon_i) = Z(U, \varepsilon_i)/Z(U, 0). \quad (13)$$

If our scaling ansatz is valid, then the $Z^*(\varepsilon_i)$ should approach a nonzero limit as $U \rightarrow U_{c2}$, i.e., they should all collapse onto a single scaling function. As shown in Fig. 3(b), this behavior is observed only for U sufficiently close to U_{c2} [note that the data for $U=0.8$ (further from the transition) show deviations from leading scaling]. This is precisely what we expect, since such simple scaling behavior typically occurs only

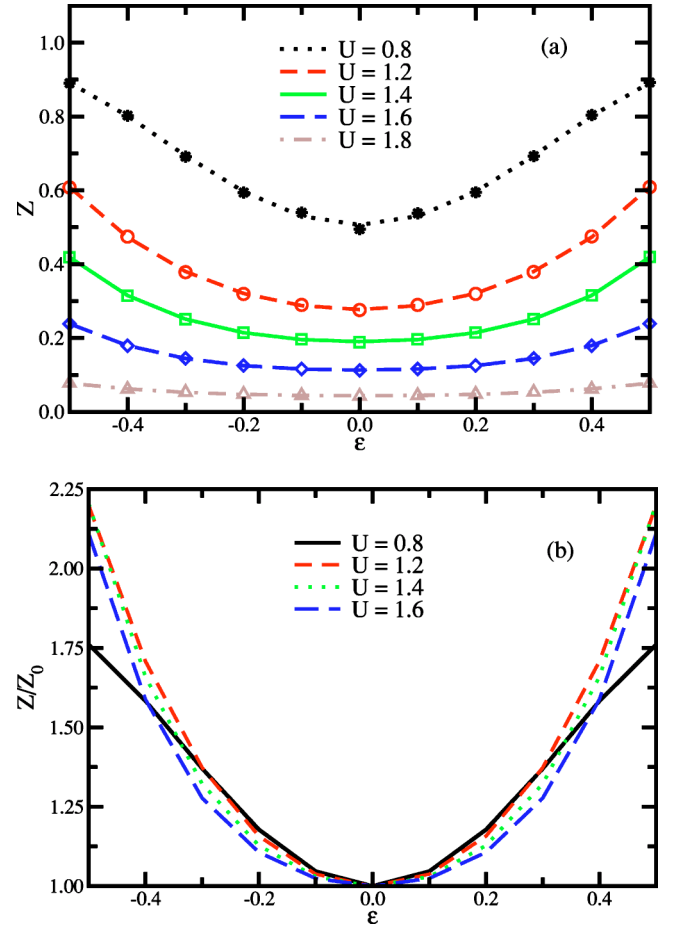


FIG. 3. (Color online) (a) Quasiparticle weight as a function of the on-site energy for different values of the interaction potential as the

line is approached, for disorder strength $W=1.0$. The symbols are the numerical data, while the lines correspond to the fitting to a function with even exponents in ε . (b) Fitted results for Z divided by Z_0 (the quasiparticle weight for $\varepsilon=0$) as a function of ε , showing that close to the U_{c2} the curves for different U scale. These results were obtained at a low but finite temperature $T=0.005$.

within a critical region close to the metallic spinodal.

B. Distribution $P(Z_i)$ of local QP weights

Equivalently, we can characterize the QP weights by their probability distribution function $P(Z_i)$. Typical results for $P(Z_i)$ are shown in the inset of Fig. 4. As the Z_i decrease near the transition, the distribution function $P(Z_i)$ changes its form and narrows down. However, if our scaling hypothesis is valid, then the *shape* of this distribution should approach a “fixed-point” form very close to the transition. More precisely, we expect the distribution for reduced QP weights $P(Z_i^*)$ to collapse to a single scaling function close to U_{c2} . Results confirming precisely such behavior are presented in Fig. 4.

An interesting question relates to the precise form of the fixed-point distribution function $P(Z_i^*)$, and how it may de-

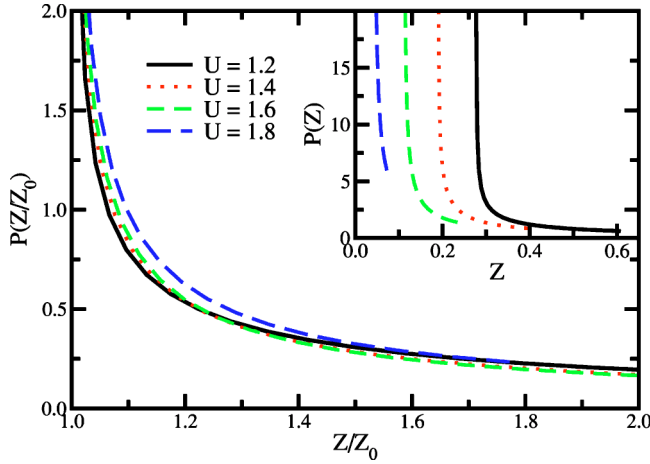


FIG. 4. (Color online) Distribution of quasiparticle weight for different values of the interaction potential. The main plot shows how the curves collapse when we look at Z/Z_0 . The inset shows the results for Z itself. Other parameters as in Fig. 3.

pend on disorder. In the clean limit, obviously, it reduces to $\delta(Z_i^* - 1)$ indicating that spatial fluctuations are suppressed. As the disorder increases, $P(Z_i^*)$ becomes very broad (as shown in Fig. 5), reflecting large site-to-site fluctuations in the local QP weights. This behavior may be regarded as a precursor of electronic Griffiths phases,¹⁷ which emerge for stronger disorder, as found within *statDMFT* approaches.¹⁰

In essential contrast to the clean limit, the approach to the Mott transition in the presence of disorder thus needs to be characterized by the entire *probability distribution function* of QP parameters. At first glance, this may appear to require a description considerably more complex than in the absence of disorder. However, we have demonstrated that in the critical region the distributions approach a fixed point form, allowing for “single parameter scaling,” in close analogy to the clean Mott transition. This finding immediately suggests that our arguments describing the finite temperature coexistence behavior in the clean limit may successfully be extended to

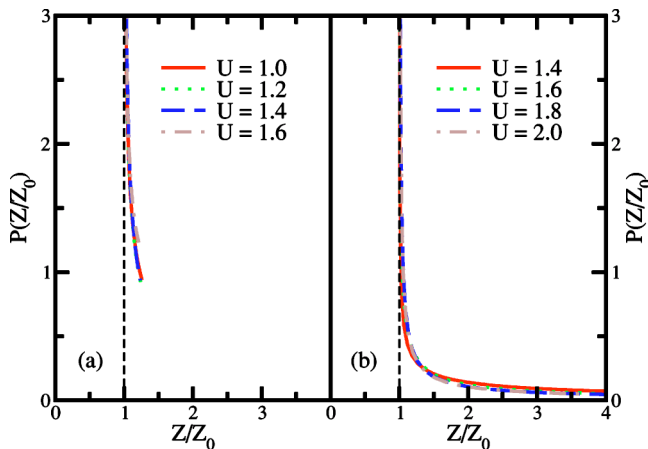


FIG. 5. (Color online) Distribution of Z/Z_0 for (a) smaller ($W=0.5$) and (b) larger ($W=1.5$) disorder than the one in Fig. 4. Other parameters used was $T=0.005$.

the disordered case as well, allowing for a complete qualitative description, which we discuss in the following section.

VI. COEXISTENCE REGION IN PRESENCE OF DISORDER

Within the DMFT formulation, the disorder is not expected to qualitatively affect the temperature dependence of the insulating spinodal, since the forms of the Hubbard bands remain qualitatively similar to that in the clean limit. The principal effect of disorder in the Mott insulating phase is to simply broaden the Hubbard bands, which retain well-defined (sharp) band edges due to the coherent potential approximation-like treatment of randomness in the DMFT limit. Indeed, our quantitative results [see Fig. 1(a)] confirm that $U_{c1}(T) \approx U_{c1}(0)$ retains very weak temperature dependence, as in the clean case. The only modification is that $U_{c1}(0)$ rapidly grows as disorder is increased, reflecting the disorder-induced broadening of the Hubbard bands.

The metallic solution is again found to be unstable above a certain coherence temperature $T^*(W, U)$, which defines the locus of the metallic spinodal $U_{c2}(T)$. An added subtlety is that different sites start to decohere at different temperatures, an effect that earlier work⁹ found responsible for a nearly linear temperature dependence of the resistivity in the disordered metallic phase. Nevertheless, sufficiently close to the Mott transition (within the coexistence region), a sharply defined temperature scale $T^*(W, U)$ emerges where the metallic solution suddenly disappears and where the qualitative form of the spectrum changes on *all* sites. This temperature scale defines the locus of the metallic spinodal, corresponding to the equation

$$T = T^*(W, U_{c2}). \quad (14)$$

At first glance, it is anything but obvious how $T^*(W, U)$ should be estimated. As in the clean case, the reduction of this temperature scale as the transition is approached must reflect the behavior of the local QP weights Z_i , and presumably depend on the precise form of the distribution function $P(Z_i)$. As we have seen, however, all the local QP weight scale in a similar fashion in the critical regime, which suggests that a reasonable estimate may be obtained simply from their average value

$$\langle Z_i \rangle = \int d\varepsilon_i P(\varepsilon_i) Z_i. \quad (15)$$

At least for sufficiently weak disorder, we may expect that [cf. Eq. (5)]

$$T^*(W, U) \approx AT_F \langle Z_i \rangle, \quad (16)$$

where $A \approx 0.2$ as in the clean case. Using the fact that all Z_i 's decrease linearly near the transition, we expect

$$\langle Z_i \rangle = C(W)[U_{c2}(0) - U]. \quad (17)$$

To confirm this, we explicitly calculated $\langle Z_i \rangle$ as a function of U for different levels of disorder; the results are shown in

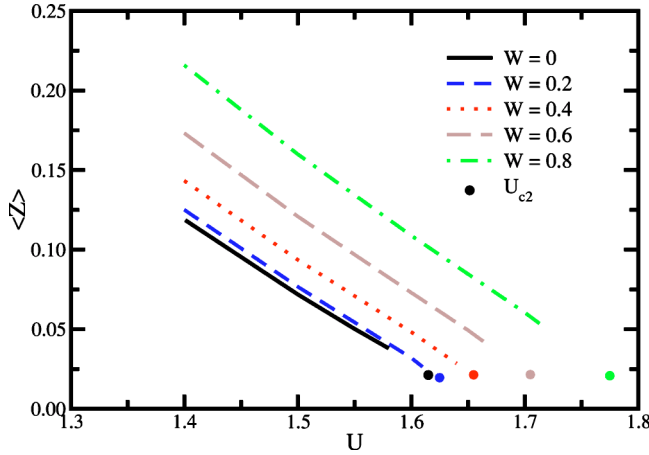


FIG. 6. (Color online) Average quasiparticle weight as a function of the interaction potential for different values of disorder.

Fig. 6. We conclude that $C(W) \approx C(0) \approx 0.45$. These results suggest that the metallic spinodal should take the form,

$$U_{c2}(W, T) \approx U_{c2}(W, 0) - B(W)T, \quad (18)$$

where $B(W) \approx B(0) = 22$. Our nonzero temperature results for $U_{c2}(W, T)$ [see Fig. 1(a)] fully confirm these expectations. Based on these results, we finally obtain the desired expression for $T_c(W)$ of the form

$$T_c(W) \approx [U_{c2}(W, 0) - U_{c1}(W, 0)]/B(0). \quad (19)$$

To test the proposed procedure, we have used the values for $U_{c1}(W)$ and $U_{c2}(W)$ at the lowest temperature of our calculation ($T=0.005$) to estimate $T_c(W)$. As we can see from Fig. 7, our analytical estimates are found to be in excellent agreement with results of explicit nonzero temperature calculations. The decrease of $T_c(W)$ with disorder thus directly reflects the “shrinking” of the coexistence region at low temperature, which in its turn reflects the decrease of the energy difference between the metallic and the insulating solution.

VII. CONCLUSIONS

In this paper, we have used a DMFT approach to examine the effects of disorder on the critical behavior near the Mott metal-insulator transition, with special emphasis on nonzero temperature properties associated with the two spinodal lines U_{c1} and U_{c2} . By using a combination of numerical results and analytical arguments, we have demonstrated that simple scaling behavior emerges, providing a complete description of the critical regime.

In contrast to the clean case, the presence of disorder requires one to examine the entire distribution of local spectral functions, $\rho_i(\omega)$, describing how the local spectra varies with position in the sample. This can be probed with scanning tunneling microscopy. Notice that the distribution function describing the site dependence of $\rho_i(\omega)$ will depend on the frequency of observation: It will be broader at higher energies [as seen in Fig. 2(b)], where a real space picture is

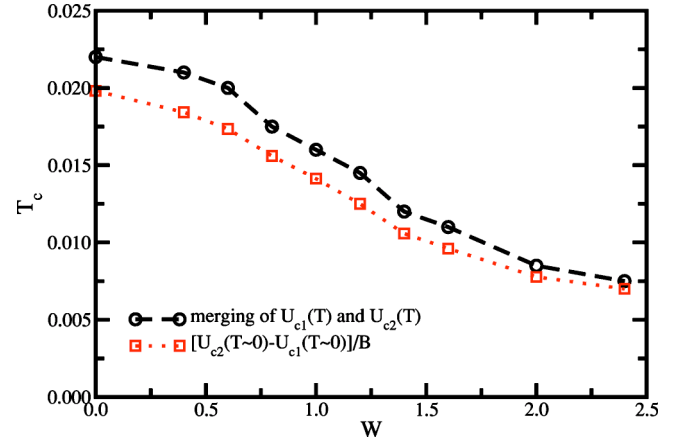


FIG. 7. (Color online) Temperature at which the U_{c1} and U_{c2} lines merge in the (U, T) phase diagram as a function of disorder. The plot shows both the results obtained directly from the numerical data as well as those calculated from the linear fitting to the $U_{c2}(T)$ line. In the latter, T_c was calculated using the values of U_{c1} at $T=0.005$, except for $W=0$ where the result at $T=0.0075$ was used.

appropriate to describe the Hubbard bands, and narrower at low frequencies, where a quasiparticle description in k space is appropriate. This is a manifestation of frequency dependence of the disorder screening discussed in an earlier paper by some of us.⁸

In the metallic regime, at low temperatures, the spectral function can be parametrized in terms of the distribution of QP parameters, which displays simple scaling properties. This allowed us to characterize the behavior near U_{c2} using a single parameter scaling procedure. The approach to U_{c2} thus retains a character qualitatively independent of the level of disorder, where the vanishing of quasiparticle weight signals the transmutation of itinerant electrons into localized magnetic moments.

Within the examined DMFT formulation, the region between the two spinodal lines U_{c1} and U_{c2} , although reduced in size and extent, cannot be completely eliminated no matter how large the disorder. Of course, these predictions are applicable only for weak enough disorder where Anderson localization effects can be ignored. Extensions of DMFT that incorporate Anderson localization mechanisms at zero temperature are available,^{10,11} but applying these approaches to examine the nonzero temperature behavior near Mott-Anderson transitions remains an interesting research direction. The behavior at the first-order transition line and the actual nucleation of either the metallic or insulating phase, between U_{c1} and U_{c2} , are also strongly modified by disorder, and this as well is left for future study.

ACKNOWLEDGMENTS

The authors thank A. Georges and D. Tanasković for useful discussions. This work was supported by NSF Grant Nos. DMR-9974311 and DMR-0234215 (V. D.) and DMR-0096462 (G. K.).

- ¹A. Georges, G. Kotliar, W. Krauth, and M. J. Rozenberg, *Rev. Mod. Phys.* **68**, 13 (1999).
- ²Y. Sekine, H. Takahashi, N. Mōri, T. Matsumoto, and T. Kosaka, *Physica B* **237**, 148 (1997).
- ³M. Matsuura, H. Hiraka, K. Yamada, and Y. Endoh, *J. Phys. Soc. Jpn.* **69**, 1503 (2000).
- ⁴S. Miyasaka, H. Takagi, Y. Sekine, H. Takahashi, N. Mōri, and R. J. Cava, *J. Phys. Soc. Jpn.* **69**, 3166 (2000).
- ⁵P. Limelette, P. Wzietek, S. Florens, A. Georges, T. A. Costi, C. Pasquier, D. Jérôme, C. Mézière, and P. Batail, *Phys. Rev. Lett.* **91**, 016401 (2003).
- ⁶C. Strack, C. Akinci, B. Wolf, M. Lang, J. A. Schlueter, J. Wosnitza, D. Schweitzer, and J. Müller, *cond-mat/0407478*.
- ⁷V. Dobrosavljević and G. Kotliar, *Phys. Rev. Lett.* **71**, 3218 (1993); *Phys. Rev. B* **50**, 1430 (1994); M. Ulmke, V. Janiš, and D. Vollhardt, *ibid.* **51**, 10 411 (1995).
- ⁸D. Tanasković, V. Dobrosavljević, E. Abrahams, and G. Kotliar, *Phys. Rev. Lett.* **91**, 066603 (2003).
- ⁹M. C. O. Aguiar, E. Miranda, V. Dobrosavljević, E. Abrahams, and G. Kotliar, *Europhys. Lett.* **67**, 226 (2004).
- ¹⁰V. Dobrosavljević and G. Kotliar, *Phys. Rev. Lett.* **78**, 3943 (1997).
- ¹¹K. Byczuk, W. Hofstetter, and D. Vollhardt, *Phys. Rev. Lett.* **94**, 056404 (2005).
- ¹²The fact that the quasiparticle parameters are site-dependent was emphasized by G. T. Zimanyi and E. Abrahams, *Phys. Rev. Lett.* **64**, 2719 (1990).
- ¹³H. Kajueter and G. Kotliar, *Phys. Rev. Lett.* **77**, 131 (1996).
- ¹⁴M. Potthoff, T. Wegner, and W. Nolting, *Phys. Rev. B* **55**, 16 132 (1997).
- ¹⁵The definition of the coherence temperature T^* used in previous estimates, was based on the temperature dependence of the resistivity. It was defined as the temperature where deviations from the low-temperature T^2 form became appreciable, and as such represents a crossover scale. That work found $A \approx 0.1$, which is in reasonable agreement with our present result $A \approx 0.2$, given the ambiguity in precisely defining the resistivity crossover scale.
- ¹⁶In addition to the quasiparticle weight, the low-energy excitations are also characterized by renormalized site energies describing the renormalized disorder potential. However, within the DMFT scheme, the renormalized disorder is strongly screened, so the local quasiparticle weights $Z(\varepsilon_i)$ are sufficient to characterize the critical behavior.
- ¹⁷E. Miranda and V. Dobrosavljević, *Phys. Rev. Lett.* **86**, 264 (2001); D. Tanasković, E. Miranda, and V. Dobrosavljević, *Phys. Rev. B* **70**, 205108 (2004).